SEBHA UNIVERSITY JOURNAL OF PURE & APPLIED SCIENCES VOL.20 NO. 2 2021
DOI: 10.51984/JOPAS.V20I2.1176

جامعة سبها للعلوم البحتة والتطبيقية مجلة
Sebha University Journal of Pure & Applied Sciences

Journal homepage: www.sebhau.edu.ly/journal/index.php/jopas

The Effects of Pits Size and Shape on Fatigue Crack Initiation

*Salah A. Gnefid[a], Robert Akid[b]

[a]Faculty of Natural Resources, Sawknah, 3Q7J+XHP, Libya
[b]School of Materials, University of Manchester, Manchester M13 9PL, UK

Keywords:
AVPP
Crack
Corrosion
Fatigue
Oxide-film

ABSTRACT

Corrosion pits were electrochemically generated on the surface of 316L stainless steel using a scanning droplet cell technique in order to assess the effects of various factors such as pit size, pit shape, solution flow rate, and applied stress on pit initiation and corrosion fatigue growth. Pit and short fatigue crack growth behaviour was monitored as a function of fatigue stress cycles to investigate the individual stages of the corrosion fatigue damage process occurring at the material surface. A comparison of virgin as-received material with samples having a modified surface film, using the alternating voltage passivation process (AVPP) has been made. The effects of corrosion on cracking behaviour during the different stages of corrosion fatigue crack growth are discussed.

تأثيرات حجم و شكل النقرات على نشؤ كسور التعب

*صالح عبدالله قنيفيد [1] و روبرت أكيد [2]

[1]كلية الموارد الطبيعية جامعة الجفرة ، سوكنة ، 3 *Q7J+XHP*، ليبيا
[2]مدرسة المواد ، جامعة مانشستر، مانشستر ، *M13 9PL* ، المملكة المتحدة.

الكلمات المفتاحية:
AVPP
الكسور
التآكل
التعب
الطبقة المؤكسدة

الملخص

استحداث و مرافبة نمو نقرات التآكل على سطح الفولاذ الغير قابل للصداء316 L باستخدام تقنية خلية ماسحة التقطير و التحقق من مدى تأثير عوامل عديدة مثل حجم النقرة و شكلها و تأثير سرعة التذفق و الأجهاد المطبق على نشؤء النقرات و نموها. و لذلك تم تجهيز منظومة لقياس سلوك النقرة و تكون الكسور القصيرة و تمددها ، لمعرفة كل مرحلة من مراحل الأنهيار بالتعب التي تحدث على سطح المعدن و مقارنتها بسلوك الأسطح المعدلة باستخدام عملية الغمر بالجهد المتردد.

Introduction:

Austenitic stainless steel materials have been used in a variety of applications where good resistance to corrosion and high mechanical strength are required. However, they are susceptible to localised corrosion in aggressive environments in particular when they are also subjected to cyclic loading [i,ii]. Therefore, the objective of industries is to enhance the resistance of these materials by introducing manufacturing techniques to modify the material surface structure and composition. Development of a homogenous oxide film is one of the objectives to obtain a novel surface function of metallic materials. Recently, the alternating voltage passivation process (AVPP) was reported to enhance the corrosion resistance of stainless steels as a result of increasing the oxide layer thickness and changing its composition [iii,iv]. Localised corrosion including pitting corrosion is classified as one of the major damage mechanisms affecting the integrity of many materials and structures in a variety of applications. Corrosion pits generally initiate due to some chemical or physical heterogeneity at the surface, such as inclusions, second phase particles, flaws, mechanical damage, or dislocations [v]. The main aim of this study was to assess the influence of AVPP treatment on the 316L SS native oxide film on the local electrochemical behaviour and the crack initiation behaviour.

Experimental Work

Material used is 316L SS with a yield stress of fatigue crack initiation 300MPa and a chemical composition as shown in Table1. Figure 1 shows the corrosion fatigue testing system which includes the Scanning Droplet Cell (SDC), the stress rig and their operating accessories. The SDC incorporates a technique which confines a liquid in contact with a sample surface in order to measure electrochemical and corrosion reactions over a limited region where the droplet is actually in contact with the sample. This offers the ability to spatially resolve electrochemical activity and to confine it

*Corresponding author:
E-mail addresses: salah.gnefid@ju.edu.ly , (R. Akid) robert.akid@manchester.ac.uk
Article History : Received 11 April 2021 - Received in revised form 12 December 2021 - Accepted 30 December 2021

exclusively to a quantifiable area of the sample. The technique which has been previously reported in the scientific literature [vi] employs a glass theta capillary to deliver the drop to the surface however in this set up we have introduced a new SDC head (image 1 in Fig.1). The counter and reference electrode are contained within the capillary block.

Pit Geometry Measurement

Volume (V), area (A) and roughness (Ra) analysis were performed using the Alicona™ IFM (Infinite Focus Microscope) to obtain the profiles of the corroded material surface. The volume obtained from these measurements was converted to weight loss W by considering the material density (ρ).

$$W = \rho V \quad [g] \qquad \text{Eq (1)}$$

A wide variety of pit growth laws have been reported [vii,viii,ix] for different metal-electrolyte systems, however these laws are based on typical corrosion cells where generation of many pits are expected. The objective of this part of the experimental work was to generate corrosion pits using the SDC and subsequently measure pit geometric using the IFM to obtain a pit growth law. Pits were generated on 316LSS samples in 3.5 wt% NaCl at pH 6.5 and room temperature. Prior to corrosion the sample surface was wet ground to 1200 grit finish and then polished to 1 µm using diamond paste. Samples were polarised at different periods typically, at 30, 60, 90,…,360 min. Pits were generated by controlling the applied anodic potential at a value around the pitting potential namely 0.5V vs saturated calomel electrode. It was possible to generate pits of different depths as were reported in the literature [x, xi, xii, xiii, xiv].

Pit Initiation and Growth

The corrosion-fatigue tests were stopped after a particular number of cycles or where noticeable changes in the current had occurred. The pit-profile generated during the corrosion- fatigue tests was measured using the IFM. A plot of pit-depth versus the number of cycles is presented in Figure 2 for the 316L SS samples and for the 316L-AVPP-treated samples. These results show that pits developed during the corrosion-fatigue tests grow gradually to a particular size for a number of cycles and then continue to grow rapidly until complete failure occurs. The maximum pit-diameter is generally equal to the SDC tip diameter which represents the droplet size. However, sometimes pit grew further to contain micro-defects generated because of cycling stress. Figure 3 shows an example of pit-growth during the corrosion-fatigue test for the 316L SS sample from 90µm diameter and 20µm depth at 5.5% of the fatigue-life (FL) to 800µm diameter and 500µm depth at about 80% (FL). The latter Fig.3b includes the main corrosion-fatigue crack.

Table 1: Chemical composition of 316L stainless steel material (wt. %).

C	Cr	Ni	Mo	Mn	Si	P	S	Co	N	Fe
0.017	16.72	10.06	2.03	1.26	0.40	0.035	0.005	0.16	0.04	69.2

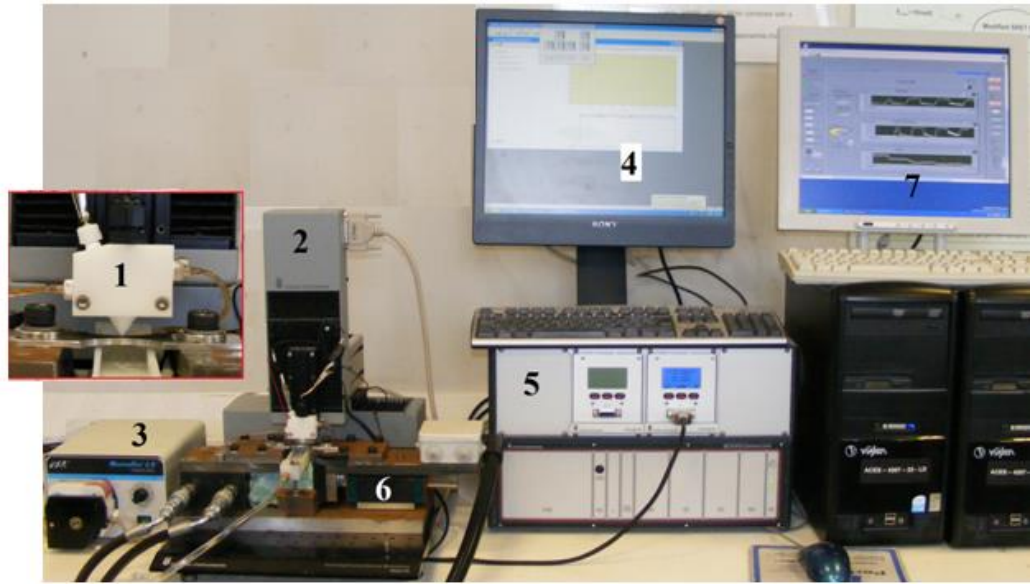

Fig.1: Corrosion Fatigue System: SDC head (1); positioning system (2); peristaltic pump (3); UniScan M370 software (4); UniScan potentiostat (5); stress rig (6); Stress cell software (7).

Results and Discussions:

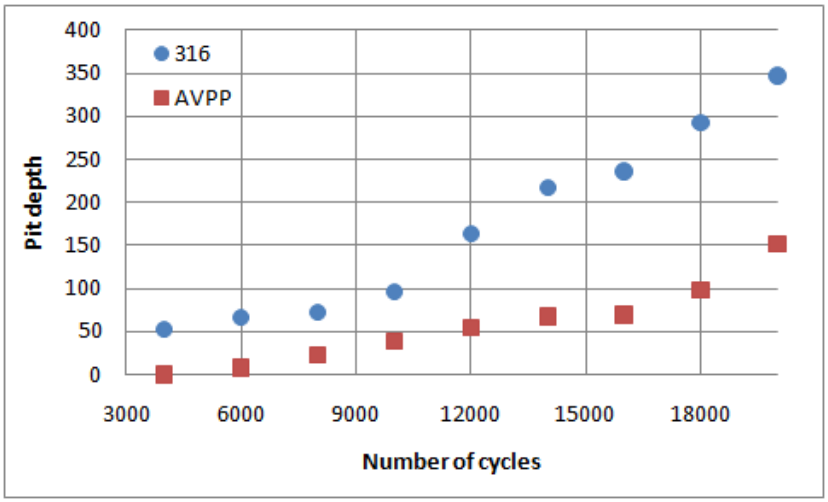

Fig.2: Pit depth vs. number of cycles for Samples 316L, and 316L with AVPP, during CF tests.

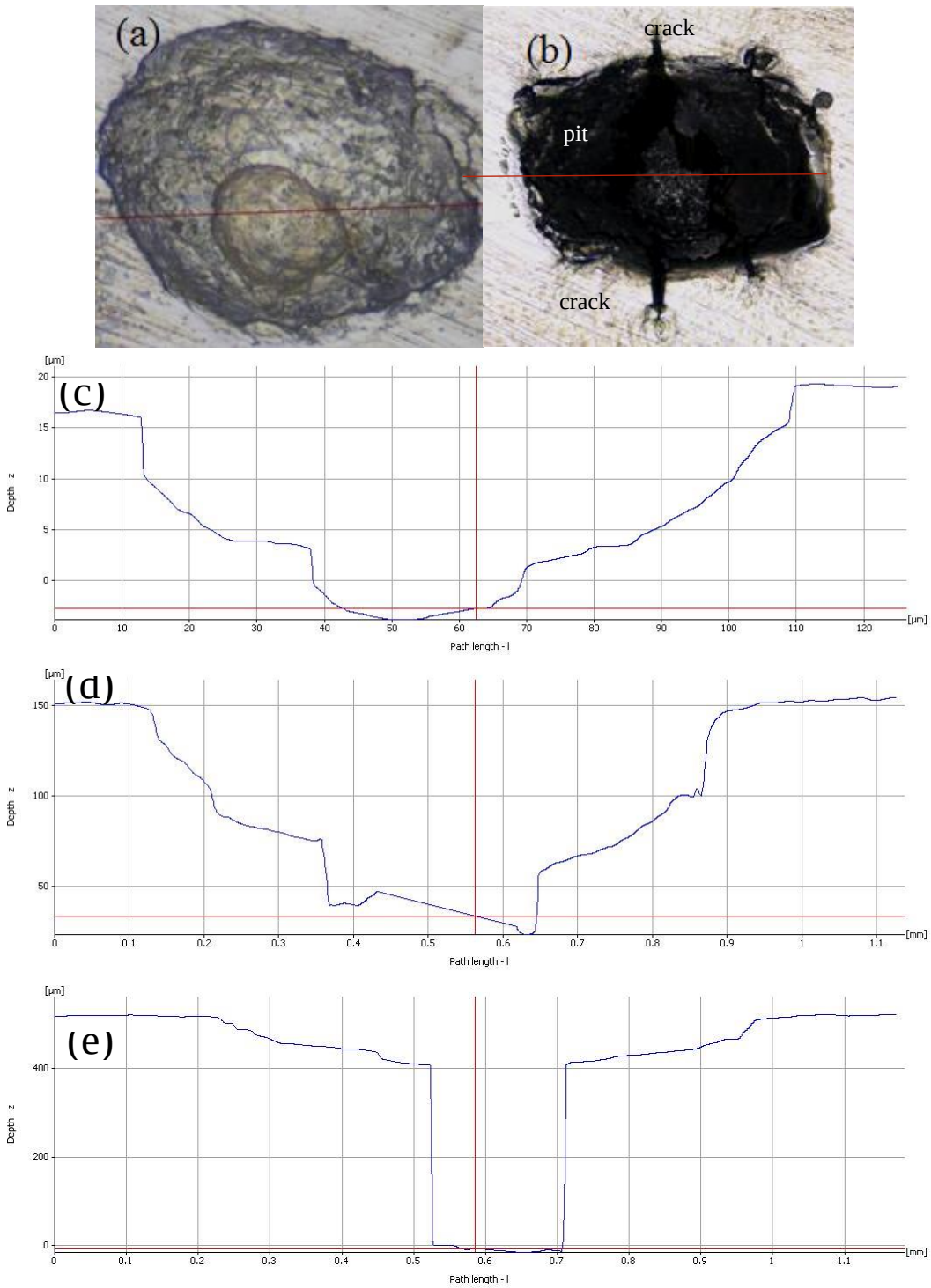

Fig.3: An optical micrographs of pit for the 316LSS Sample during CF tests at (a) 5.5% FL(22,600 cycles) and (b) at 90%FL. It is growth profile (c) at 5.5% FL, (d) at 67%FL and (e) at 90%FL.

Corrosion Fatigue Crack Initiation and growt

This section represents the results of the corrosion-fatigue tests which were conducted for 316L SS and 316L-AVPP-treated at a stress level of 260MPa (87% of yield stress). These results include the crack growth which was obtained from Infinite Focus Microscope images. This optical microscope allows the measurement of pit-profiles and cracks, and the taking of 3D images. Corrosion-fatigue cracks for both surfaces tested behaved in a similar growth manner regardless of the delay in crack-initiation which was caused by the delay in pitting for the 316L-AVPP-treated samples. Crack initiation was associated with a localised electrochemical pitting-process. As cycling continued, pits grew in diameter and in depth, resulting in the formation of a stress concentration site. It was found that micro-cracks were initiated at two locations. Notably some micro-cracks were initiated inside the pits and others were initiated at the perimeter of pits each side of the pit at 90o to the loading axis. Figure 4 shows the process of initiation and propagation of a corrosion- fatigue crack inside a pit generated by SDC. Those micro-cracks that initiated inside the pit were propagated to form a main crack which developed outside pits and led to failure.

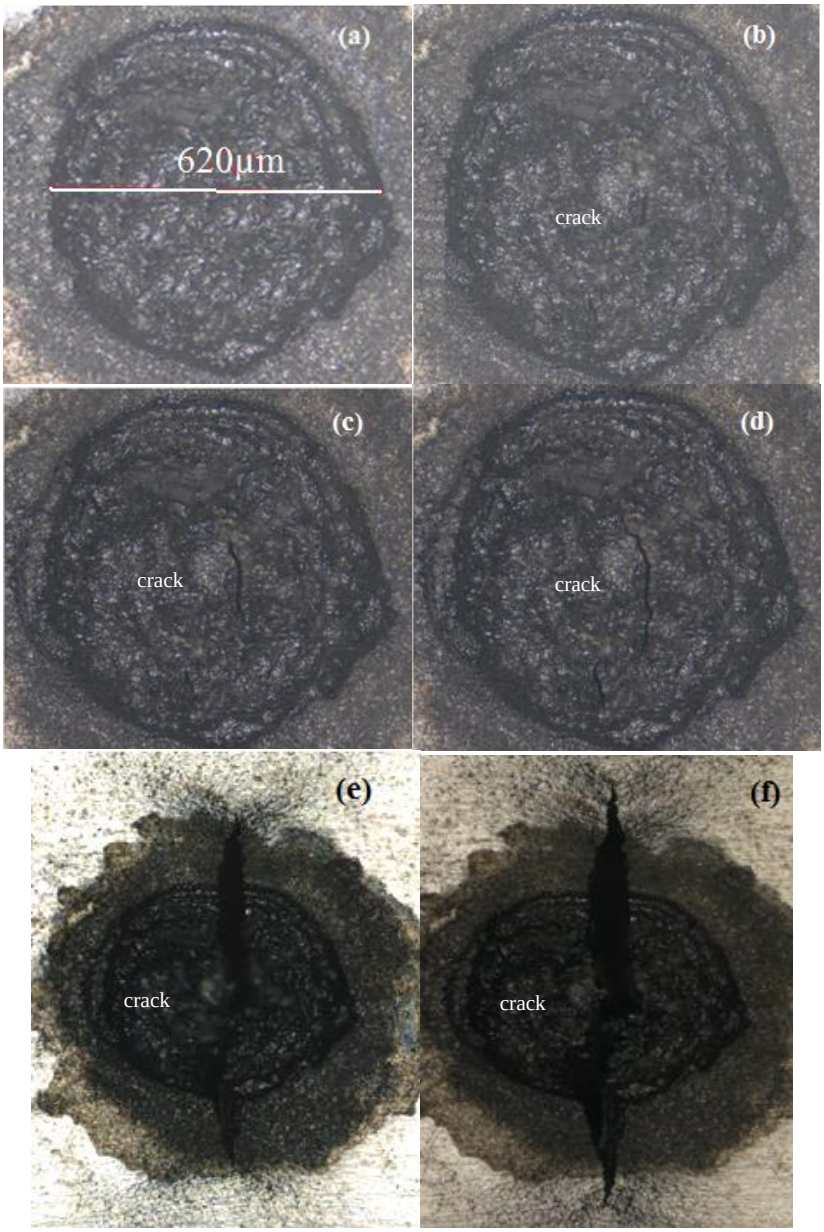

Figure 4: The corrosion-fatigue crack initiation and propagation process associated with corrosion pits, 260 MPa, 3.5% NaCl solution (a) 30% , (b) 35% (c) 45%, (d) 62%, (e) 76% and (f) 85% of fatigue-life.

It appears that intergranular corrosion took place inside the pits at the grain-boundaries; as cyclic loading continued, these grain-boundaries formed micro-cracks see Figure 5. These micro-cracks were due to a combination of stress and corrosion. The main crack grew from both sides of the pit at 90º to the tensile axis (mode I) and the crack growth was perpendicular to the applied load direction. The crack growth continued to final failure after overcoming the microstructural barriers for example grain-boundaries. When the crack encountered these barriers, the crack direction changed, forming two branches (secondary cracks) and producing a large plastic deformation zone. However, due to the fact that resolved stress is lower acting on the secondary cracks, overall propagation of the crack remained at 90º to the tensile axis (mode I) as can be seen in Figure 6.

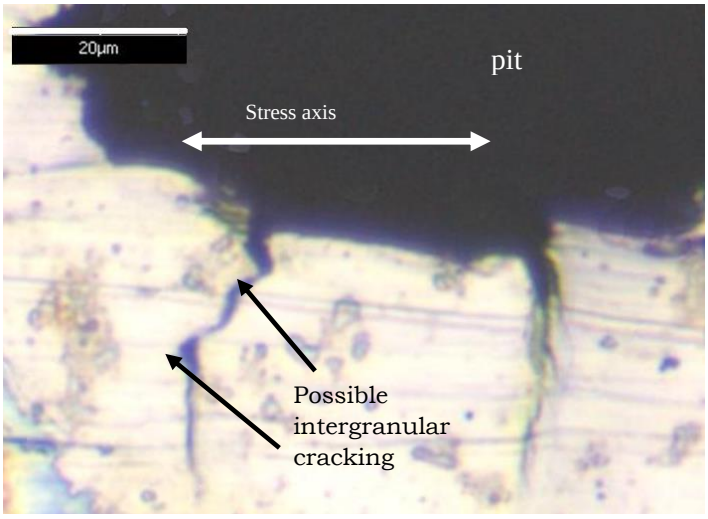

Fig.5: Corrosion-fatigue crack initiation associated with corrosion pit, 260 MPa, 3.5% NaCl solution at 45% of fatigue-life.

The other observation of crack initiation that has been observed is crack initiation from the pit as can be seen in Figure 5. In some cases dissolution caused blunting of the cracks leading to crack arrest. The dissolving of the micro-cracks led to a widening of the pit, and as a result decreasing the stress-concentration produced from the pit. Other cracks which continued to grow outside the pit were subjected to retardation of their growth because of grain-boundary barriers. As can be seen from Figure 6, this retardation resulted in the formation of large plastic zones after which cracks continued their growth. In the first type of crack initiation, it was seen that the crack grew from the inside of the pit to the outside until failure. However in the second type, two major cracks were initiated at the edges of the pit; and these grew perpendicularly to the applied stress outside the pit to a particular size prior to coalescence. Before coalescence, the two main cracks grew towards the pit-centre assisted by dissolution of the growing crack see Figure 4. Crack growth behaviour was studied by measuring crack-length corresponding to a particular number of applied loading cycles. After collecting data from a test, a plot of surface crack-length versus fraction of fatigue life was obtained, as shown in Figure 7.

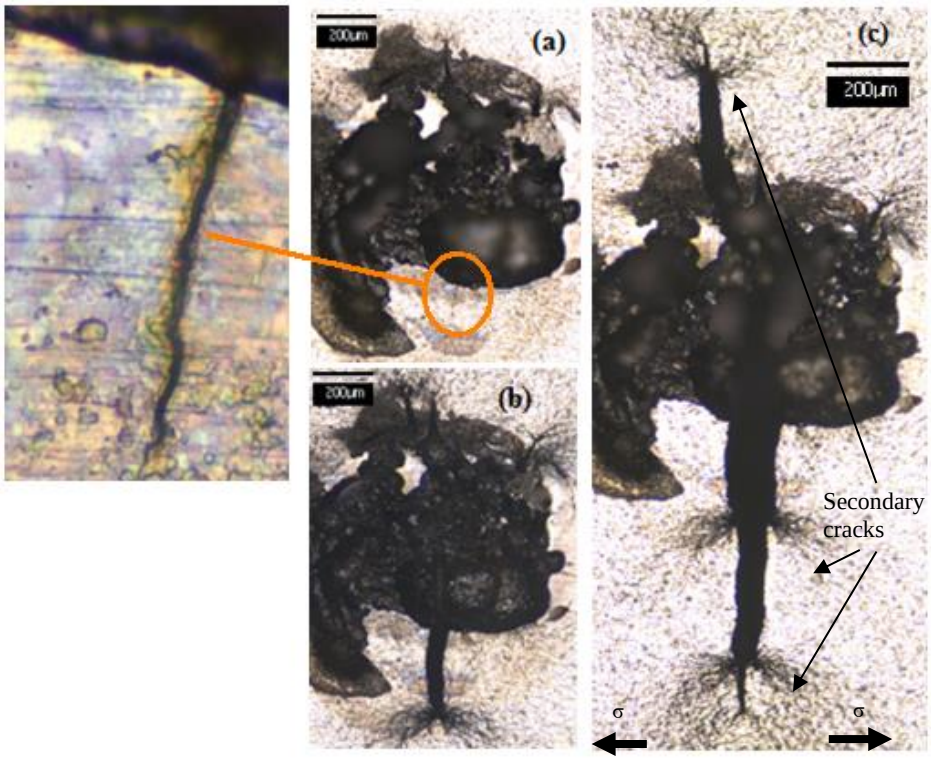

Fig.6: The Corrosion-fatigue crack initiation and propagation process in association with corrosion pit, 260 MPa, 3.5% NaCl solution (a) 45% , (b) 62% and (c) 93% of fatigue-life.

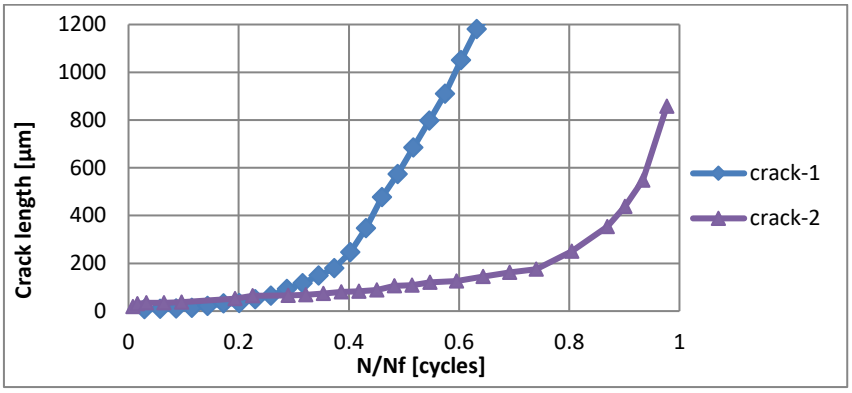

Figure 7: Corrosion-fatigue crack- length vs. fraction of fatigue life for the 316L SS Sample.

Once initiated, micro-cracks from the end of a pit propagated in mode I perpendicular to the applied load axis. Initially these cracks showed high growth rate followed by deceleration in growth as they reached a grain boundary. After overcoming the first grain boundary cracks accelerated and showed another deceleration in growth on reaching the next grain boundary. This behaviour was repeated several times (6 or 7 grains as grain size was estimated to be 23µm) [xv] and they shown in Figure 8. The effect of microstructure was noted up to around 160µm after which cracks increased in crack growth rate up to complete failure of the sample.

However, when cracks initiated in the pit bottom less retardation behaviour was observed as shown in Figure 8 (crack1). This difference in growth behaviour may be caused by the difference in the environmental conditions for the two cracks. Cracks initiated inside the pit their growth enhanced by electrochemical dissolution because of low solution pH. However cracks outside pits grew in dry condition i.e. not in contact with SDC droplet

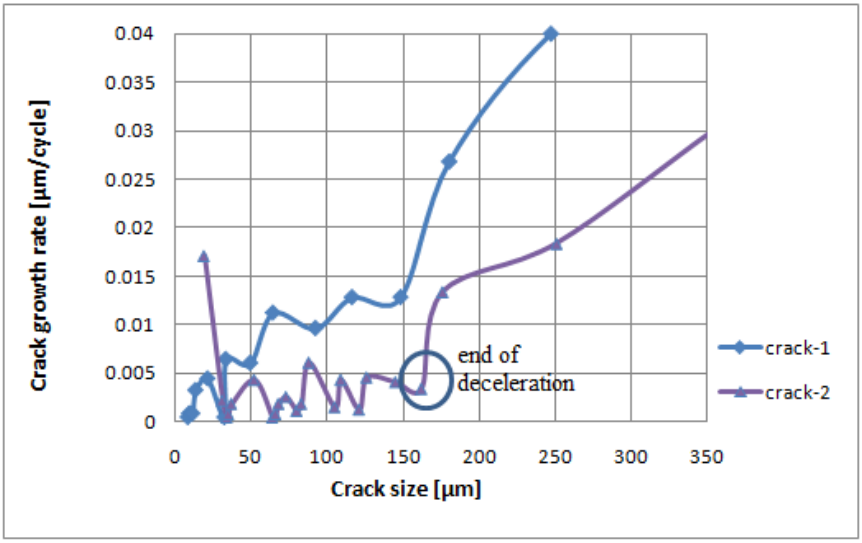

Figure 8: Crack growth-rate vs. crack size for crack-1 inside a pit, crack-2 outside a pit.

Fracture Surface Morphology

The fatigue fracture surface morphology of 316L specimens tested using SDC in 3.5%NaCl solution is shown in Figure 9. Approximately 75% of the fracture surface appeared relatively smooth and associated with a ductile growth of fatigue crack stage I and stage II. The remaining 25% of the surface had a rough texture associated with the final brittle fracture of the sample. Noticeable deformation of the sample exists in the area of final failure. On the fracture surface, secondary cracks were observed from the main crack that led to failure. It is worth noting for all the testing samples that all the cracks were initiated from corrosion pits.

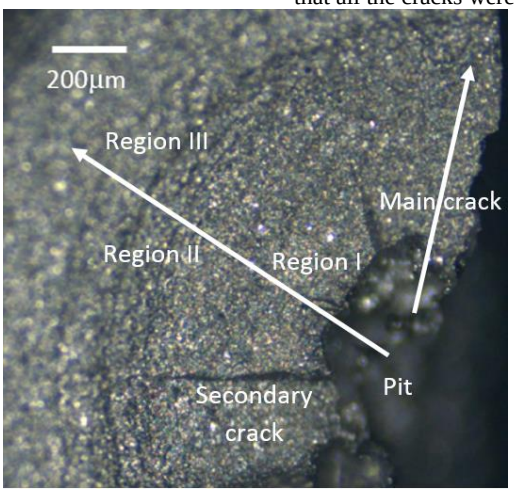

Figure 9: IFM fracture surface morphology for 316L SS after corrosion fatigue test, the axial tensile cycling loading direction is perpendicular to the image.

Pitting Behaviour and SDC Studies

To further understand the mechanism of pitting corrosion in stainless steel alloys the scanning droplet cell (SDC) technique was used to generate corrosion pits under controlled potential. The use of microcapillary techniques in the evaluation of localised corrosion has been previously reported [xvi,xvii,xviii,xix,xx,xxi]. In the case of the SDC studies presented here, the pit profiles for a given flow rate, surface finish and applied static stress was measured using an infinite focus microscope. Typical pit profiles obtained by this technique are shown in Figure 10. The shape of the removed material in Figure 10a was a circular groove which appears dark in the image because of the difference in depth.

The central area inside the circle appears to form an island which includes intact surface with disruption of few undeveloping pits this is clearly seen in Figure 10a. This phenomenon was reported in other work [xxii]. It is noteworthy that the groove formed varies in depth, where the groove at the solution inlet side is deeper than at the outlet side. This behaviour is considered to be the result of increased availability of oxygen, and subsequent increased dissolution, on the inlet side.

Furthermore it might be reasonable to assume that the actual flow dynamics are slightly different on the inlet and outlet sides, with the outlet side being somewhat more quiescent.

However, the pits shown in Figure 10b,c,d are typical of those observed in tests. The cross-section of this kind of pit having a large diameter on the surface and becoming gradually more narrow towards the bottom of the pit to give a (V) shape and in some cases a (U) shape.

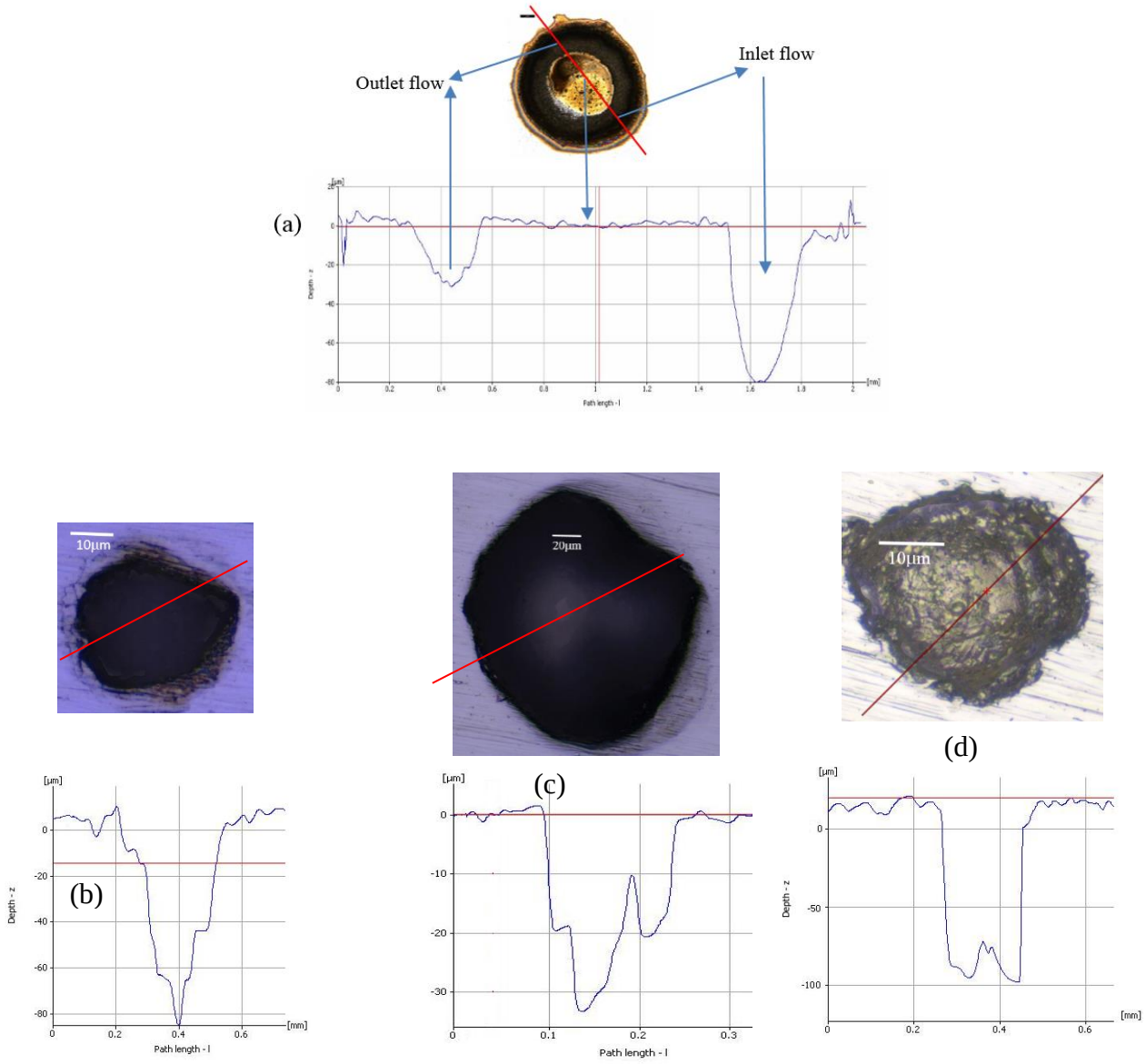

Figure 10: Typical profiles of pits generated on 316L SS surface using SDC in 3.5wt%NaCL, obtained by IFM

An understanding of the mechanism of pit growth is generally achieved by conducting electrochemical or metallographic methods, however a combination of the two methods is usually preferred. Figure 11 represents results from SDC tests in term of material weight, as calculated using Faraday's law, compared to weights calculated from the volume of material removed measured using IFM. In the low flow rate regime (below 25 mm^3/s) there is reasonable correlation between the SDC and IFM results. However, when higher flow rates were applied the difference between the two results increased. Pits produced at low flow rates were found to be shallower than pits produced from higher flow rate. Deeper pits are more difficult to measure due to the onset of undercutting of the pits and this inability of IFM to measure undercutting due to line of sight measurements.

In electrochemical measurements, the value of the flow rate is important as flow plays an important role in transporting oxygen and active species to the metal surface and promotes the removal of the products of corrosion away from the site thereby changing the diffusion characteristic of the corrosion cell. In this study for the set electrochemical conditions, it was found that the current density increases with the increase in flow-rate. It has already been suggested

that increasing the flow rate increases the rate of oxygen release from the electrolyte to the metal surface which increases the rate of corrosion [xxiii]. Krawiec et al. [xxiv] studied the parameters responsible for affecting the mass transport and the distribution of species in micro-capillaries close to the specimen surface, they reported enhancement in cathodic current with increasing electrolyte flow rate. However in a previous study [xxv] it was found that there was no effect on corrosion rate of 304 stainless steel when the flow velocity of natural water containing ozone increased from 0.05 to 1.7 m/s. However, the pitting potential was decreased in a potentiodynamic scan test when the flow rate increases for same material in 3.5% NaCl [xxvi]. It was found that enhanced dissolution at the metal surface occurred during the application of stress, and it was suggested that plastic deformation created areas from which dissolution of atoms occurred more readily than that from the relatively unstrained surface. This can be seen in Figure 12 where pit depth developed in an unstressed sample compared to that obtained from a corrosion fatigue sample. Based on the size of the pit at the crack-pit transition the stress concentration threshold factor range for 316L on corrosion fatigue using SDC technique, was found to be from 2.1 to 2.5 MPa√m [15].

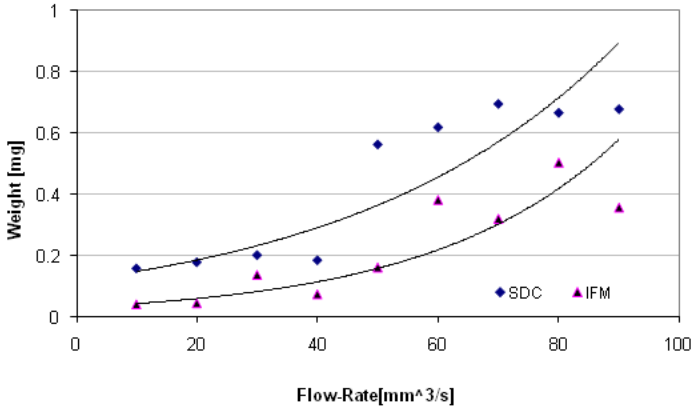

Figure 11: Weight of material removed as calculated from Faraday's law using SDC current-time measurements and as measured with IFM.

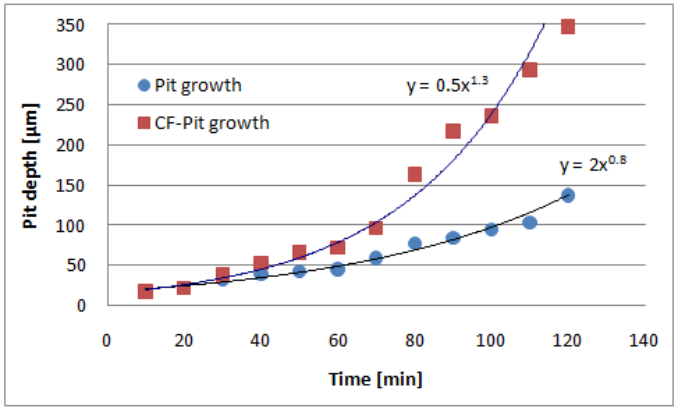

Figure 12: Pit depth vs. time for Samples 316L, with (CF-pit growth) and without cycling loading (pit growth).

Conclusions:

The original surface film of 316L austenitic stainless steel was modified electrochemically using an alternative voltage passiviation process (AVPP) to study the effects of this modification on the crack initiation and corrosion properties. The effect of applied surface stress on the development of corrosion pits has been assessed in relation to their role on the fatigue behaviour of stainless steel materials, in particular the early stages of corrosion fatigue. Several experimental techniques have been used to quantify changes in material response during stress and corrosion interactions. The effect of corrosion pits on the fatigue behaviour of stainless steel materials in particular the short crack regime was investigated using the SDC in combination with a fatigue rig. Results showed an improvement in the corrosion fatigue life in the AVPP modified 316L SS surface compared to the native surface due to a delay in film breakdown and pit initiation.

References

[1]- Rezig E. Irving P.E., Robinson M.J. "Development and early growth of fatigue cracks ….", (2010) Science Direct, Procedia Engineering 2 (2010) 387-396.

[2]- Alan Turnbull, "Corrosion pitting and environmentally assisted small crack growth", (2014) Proceeding of Royal Society, Volume 470.

[3]- Vignal, V. ; Valot C., ; Oltra R., ; Verneau M., ;. Coudreuse L "Analogy between the effects of a mechanical and chemical perturbation on the conductivity of passive films" Corrosion Science **44** (2002), 1477–1496.

[4]- Mansfeld, F; Lin, S.; Kwiatkowski, L. "The effects of process parameters on alternating voltage (AV) passivation of 304SS", Corros Science 34 (1993). 2045-2058.

[5]- Pidaparti R., Patel R. "Investigation of a single pit/defect evolution during the corrosion process" Corrosion Science 52 (2010) 3150–3153.

[6]- Lohrengel M. M., · Moehring A. and· Pilaski M., "Electrochemical surface analysis with the scanning droplet cell". Fresenius J Anal Chem (2000) 367 :334–339.

[7]- Kondo Y., "Prediction of Fatigue Crack Initiation Life based on Pit Growth", (1989) Corrosion Science Vol. 45, No. 1, 7.

[8]- Miller K. J. and Akid R. "The Application of Microstructural Fracture Mechanics to various Metal Surface States.'', (1996), Proc. R. Soc. Lond. A, 452, 1411.

[9]- Akid R. & Miller KJ. "Short Fatigue Crack Growth Behaviour of a Low Carbon Steel Under Corrosion Fatigue Conditions" (1991) Fatigue Fract. Engng. Mater. Struct. Vol 4. 637.
[10]- Gonzales-Sanchez J., "Corrosion fatigue initiation in stainless steels" (2002) Ph.D. Thesis, Sheffield Hallam University.
[11]- Zhou, S. and Turnbull, A. "Influence of pitting on the fatigue life of a turbine blade steel". (1999) Fatigue Fract. Eng.Mater. Struct., 22, 1083–1093.
[12]- Zhou S. and Turnbull A., "Development of a pre-pitting procedure for turbine disc steel". British Corrosion J. **35** 2 (2000), 120.
[13]- Zhang, X., Li, S., Liang, R., & Akid, R. (2013, June 16) Effect of corrosion pits on fatigue life and crack initiation. Presented at the 13th International Conference on Fracture, Beijing, China (3), Red Hook, NY: Curan Associates, Inc.
[14]- Kolawole S. K., Kolawole F. O., Soboyejo A. B. O.& Soboyejo W. O.|Manoj Gupta "Modeling studies of corrosion fatigue in a low carbon steel" (2019) Cogent Engineering, Volume 6, 2019, Issue 1.
[15]- Gnefid S. "Initiation & Growth of Corrosion Fatigue Crack for AVPP Treated Stainless Steel" (2011), PhD. Thesis, Sheffield Hallam University.
[16]- Krawiec H., Vignal V. and Akid R., Electrochimica Acta. Vol 53 (2008). 5252-5259.
[17]- Akid R., Roffey P., Greenfield D. and Guillen D. "Local probe techniques". Woodhead Publishing Limited, Cambridge (2007), 23-32.
[18]- Suter T. and Böhni H., "A new microelectrochemical method to study pit initiation on stainless steels" (1997) Electrochim. Acta 42, p. 3275.
[19]- Vignal V., Oltra R., and Josse C., (2003) Scripta Materialia, 49, 779-784.
[20]- Vignal V., Mary N., Oltra R., and Peultier J., (2006) Journal of the Electrochemical Society, 153 (9), B352-B357,
[21]- Vignal V., Mary N., C. Valot, R. Oltra, and L. Coudreuse, Electrochemical and Solid-State Letters, 7(4), 39-42, 2004.
[22]- Sri Hastuty, Atsushi Nishikata, Tooru Tsuru. "Pitting corrosion of Type 430 stainless steel under chloride solution droplet". (2010) Corrosion Science 52, 2035–2043.
[23]- Brown B.E., Lu H.H., and Duquette D. J., (1992) Corrosion 48, P.970.
[24]- Krawiec H., Vignal V. and Akid R. "Numericalmodelling of the electrochemical behaviour of 316 stainless steel based upon static and dynamic experimental microcapillary-based techniques: effect of electrolyte flow and capillary size", (2008) Surf. Interface Anal.; 40: 315–319.
[25]- Matsudaria M., Suzuki M. and Sato Y.**"** Investigation of Carbon Steel Passivation Behavior in Deionized Water by Ellipsometry", Corrosion (1981), 37 (5): 267-270.
[26]- Mansfeld F., Kenkel J.V., **"**The Effect of Rotation on Pitting Behavior of Aluminum and Stainless Steel", Corrosion 35 (1979), P. 43.